Journal of Power Sources 187 (2009) 591–598

Contents lists available at ScienceDirect

Journal of Power Sources

journal homepage: www.elsevier.com/locate/jpowsour

Plasma-assisted deposition of lithium phosphorus oxynitride films: Substrate bias effects

Yoon Gu Kim*, H.N.G. Wadley

Department of Material Science and Engineering, University of Virginia, 395 McCormick Road, Charlottesville, VA 22904, USA

ARTICLE INFO

Article history:
Received 28 August 2008
Received in revised form 7 November 2008
Accepted 7 November 2008
Available online 27 November 2008

Keywords:
Lithium phosphorus oxynitride (Lipon)
Substrate bias
Plasma-assisted directed vapor deposition (PA-DVD)
Hollow cathode plasma

ABSTRACT

Lithium phosphorus oxynitride (Lipon) films have been synthesized by a plasma-assisted directed vapor deposition (PA-DVD) approach. In this approach, a hollow cathode technique was used to create an argon plasma through which was propagated an electron-beam generated Li_3PO_4 vapor entrained in a N_2-doped helium gas jet. Without plasma assistance, amorphous, mud cracked and highly porous Li_3PO_4 films were formed. When plasma-assistance was used, nitrogen was incorporated creating a Lipon film whose composition, morphology, structure, and deposition rate could be manipulated by modifying the substrate bias. Films with spiral or very smooth surfaces could be made in this way. Fully amorphous films or films with locally crystallized regions in an amorphous matrix could be synthesized by varying the bias voltage. The presence of these local regions of crystallinity within a Lipon film decreased the Li-ion conductivities from the 10^{-7} S cm^{-1} to 10^{-10} S cm^{-1} range.

© 2008 Elsevier B.V. All rights reserved.

1. Introduction

Solid state, thin-film batteries have attracted considerable interest for on-chip power supply applications, for incorporation in some MEMS devices and as a power source for implantable medical devices [1]. Rechargeable batteries based upon the lithium ions are of particular interest because of their high energy-specific storage density [2]. This storage density is controlled by the cathode composition and structure [3,4]. Lithiated transition metal oxide cathode materials such as $Li_{1-x}CoO_2$ can have theoretical specific storage capacity as high as 137 mAh g^{-1} [5]. During the charge/discharge cycle of a rechargeable Li/Li-ion battery, lithium ions must reversibly migrate between the cathode and a lithium anode through an electrolyte. A high Li-ion conductivity electrolyte with a high electron resistance is desirable to reduce internal voltage losses during discharge [6]. Lithium phosphorus oxynitride (Lipon) electrolytes have attracted significant interest for this application because they are stable when placed in contact with a lithium anode and can have a Li-ion conductivity in the 10^{-6} to 10^{-7} S cm^{-1} range provided they are synthesized under appropriate conditions [7].

Lipon films with suitable Li-ion conductivities for electrolyte applications are usually synthesized by RF-magnetron sputtering [7–10]. However, the low deposition rate (~2 nm min^{-1}) results in prolonged deposition times (it can take up to a day to synthesize the 1–2-μm thick films of practical interest) [8]. This has stimulated many investigations of various other deposition approaches including pulsed laser deposition (PLD) [11], electron beam evaporation [12], and ion beam-assisted deposition (IBAD) [13]. However, in some cases, they suffer from a similarly slow deposition rate and in others result in too low a Li-ion conductivity. None has yet provided a fully satisfactory route for the deposition of Lipon films for thin-film battery applications.

Recently, a plasma-assisted directed vapor deposition (PA-DVD) approach has been investigated for the rapid synthesis of Lipon films [14]. The PA-DVD approach uses an electron beam to vaporize a Li_3PO_4 target placed in the throat of an annular gas jet forming nozzle. A sufficient pressure difference is maintained across the nozzle to enable the formation of a supersonic gas jet. The jet entrains the vapor atoms and transports them to a substrate where a Li_3PO_4 film can be deposited. If the jet diameter is adjusted to match that of the substrate, the deposition efficiency can be very high resulting in a rapid deposition rate [15]. The gas jet can be doped with N_2 and a plasma used to activate the nitrogen enabling its incorporation into the film [14]. This PA-DVD approach has enabled the growth of Lipon films at more than 45 times the fastest deposition rates reported for the RF-magnetron sputtering approach [14]. Increasing the number of nitrogen ions in the plasma was found to significantly increase both the Li-ion conductivity and density within the films [16]. The substrate upon which deposition occurs can be attached to a power supply and a bias voltage applied during deposition. This can significantly modify the flux and impact energies of the depositing species.

* Corresponding author. Tel.: +1 434 982 5035 fax: +1 434 982 5677.
E-mail address: ygk4x@virginia.edu (Y.G. Kim).

0378-7753/$ – see front matter © 2008 Elsevier B.V. All rights reserved.
doi:10.1016/j.jpowsour.2008.11.070

When a negative bias voltage is applied during plasma-assisted deposition, positive ions in the vapor near the substrate are electrostatically attracted and accelerated towards the film surface across a plasma sheath [17]. Mattox used a related ion plating technique to investigate the effects of a negative bias [18]. Ion plating was found to improve film density, film morphology and film adhesion [19]. Zywitzki et al. [20] implemented a hollow cathode arc discharge technique in an e-beam physical vapor deposition (PVD) approach and found that a substrate bias modified the morphologies of Al_2O_3 films from a porous columnar structure to one that was column-free and fully dense. The use of a substrate bias also led to the growth of Al_2O_3 phases that are usually only formed at much higher deposition temperatures.

Here, we investigate the effects upon Lipon film composition and structure of applying a negative substrate bias during the deposition of thin films. We find that because of the increased surface atomic mobility, the pore content was reduced as the bias potential was increased. However, this was accompanied by the appearance of crystalline phases with a reduced Li-ion conductivity.

2. Plasma-assisted directed vapor deposition

The plasma-assisted directed vapor deposition approach uses a high voltage electron beam to rapidly evaporate atoms from the surface of a source rod located in a water-cooled crucible, Fig. 1. The evaporant is entrained in a nitrogen-doped helium gas jet created by maintaining the upstream pressure of an annular nozzle (P_u) much higher than that in the deposition chamber (P_d). When the P_u/P_d ratio of the up and downstream pressures is greater than two, a supersonic gas jet can be created. Vapor entrainment in this jet is optimized by use of an annular nozzle around the vapor-emitting tip of a source rod. The vapor atoms could be highly focused to match the substrate diameter by increasing the upstream pressure. This then enabled a high material utilization efficiency and rapid rate of film growth [15]. The use of a low vacuum (in the 0.1-Torr range) during deposition results in a high fraction of oblique vapor atom impacts with the growth surface and the films therefore had a porous columnar structure [15]. This porosity can be reduced by employing a hollow cathode plasma technique to provide an energetic, reactive deposition environment that facilitates significant atomic reassembly on the growth surface. The hollow cathode arc discharge used here utilizes a high density ($\sim10^{12}$ cm^{-3} compared to that of $\sim10^{10}$ cm^{-3} for a RF-discharge) of low voltage (3–15 eV) electrons to partially ionize the vapor and an argon working gas, Fig. 2 [21–23].

3. Experimental methodology

3.1. Thin-film growth procedure

Cold pressed 1.3 cm diameter Li_3PO_4 evaporation source rods were synthesized from a powder supplied by Plasmaterials Inc. (Livermore, CA). The electron beam evaporated Li_3PO_4 vapor was reactively deposited with plasma-activated nitrogen to form Lipon using an hollow cathode plasma technique with variable substrate bias, Fig. 2 [14,16]. A negative bias voltage was applied to a metallic substrate holder to which was attached a silicon substrate. The ambient temperature resistivity of the silicon was $18 \pm 4\,\Omega$ cm. The vacuum chamber was evacuated down to 1×10^{-2} Torr and a nitrogen-doped helium gas jet with a flow rate of 5.0 slm was formed around the Li_3PO_4 source rod. The helium flow rate was 4.5 slm while that of the nitrogen was 0.5 slm. This increased the

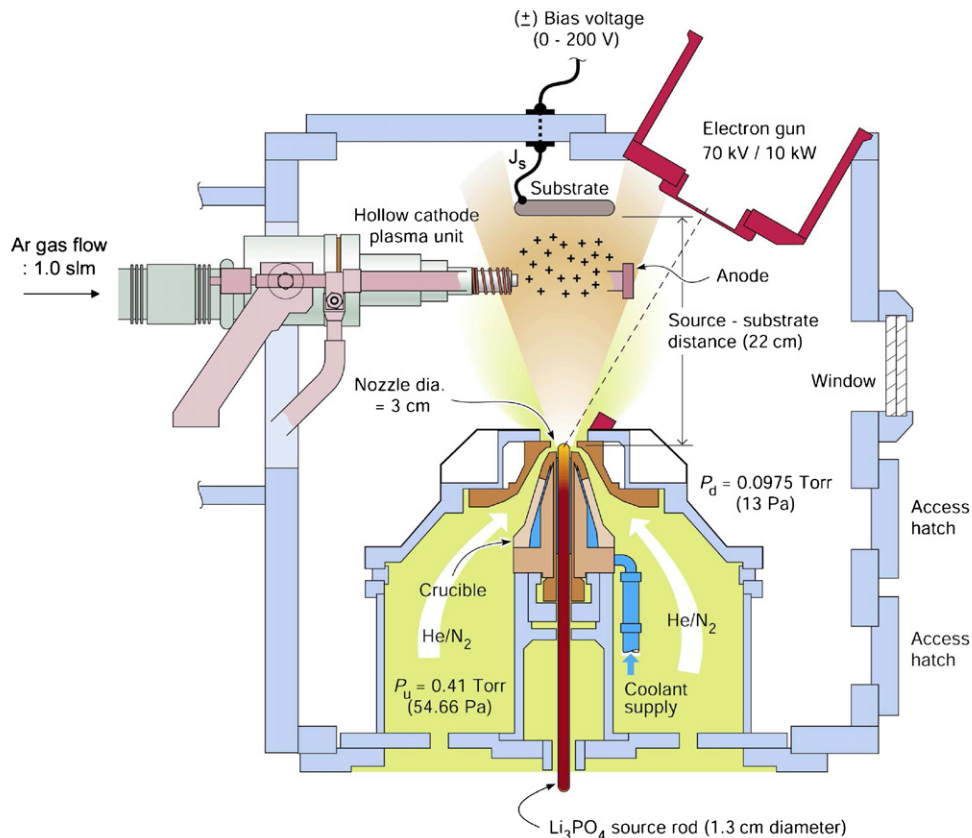

Fig. 1. Schematic illustration of the plasma-assisted directed vapor deposition (PA-DVD) process. Note that P_u denotes the upstream pressure and P_d is within the deposition chamber. During film deposition, a transonic He + N_2 gas jet was formed at the exit of an annular nozzle surrounding the evaporation source. A hollow cathode technique was used to form a plasma near the substrate.

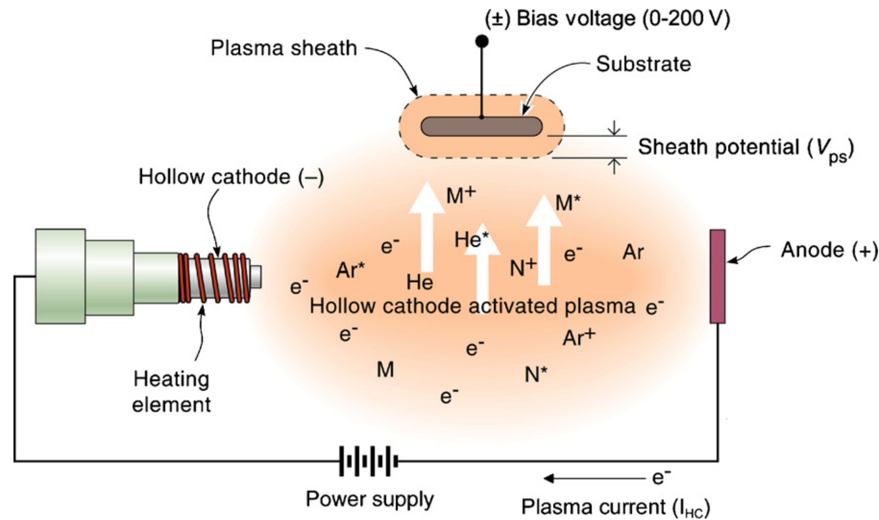

Fig. 2. Illustration of the hollow cathode plasma activation process. The hollow cathode thermionically creates a low-voltage electron beam (LVEB) with the electron energies in the 3–15 eV range. These electrons are emitted with an argon working gas from the end of the cathode and travel towards an anode plate. The plasma is formed by electron collisions with the working gas, the He/N_2 gas jet and the evaporant. This plasma contained electronically excited and ionized source vapor and working gas atoms/molecules. A negative bias voltage was applied to the substrate resulting in the formation of a plasma sheath near the substrate. The plasma sheath potential (V_{ps}) accelerated a positive ion flux towards the deposition surface. In the sketch, M represents vapor atoms/molecules, M^* represents excited vapor species, and M^+ represents ionized vapor.

downstream pressure (P_d) to 2.3×10^{-2} Torr while the upstream pressure (P_u) to 9.8×10^{-2} Torr. The pressure ratio (P_u/P_d) was 4.2, which resulted in a jet speed of ~2120 m s^{-1} at the nozzle opening [15]. An argon hollow cathode plasma was activated using a low voltage electron beam (LVEB) with a plasma current of 60 A. Lipon films were grown by evaporation of the Li_3PO_4 source using an electron beam power density of ~110.6 W cm^{-2}. Films were grown in 20–40 min at 180 ± 20 °C using negative bias voltages of 0, 10, 20, 30, and 50 V.

3.2. Incident ion flux

Prior to Lipon film synthesis, the incident ion flux upon the substrate was measured, Fig. 3 [14]. The floating potential (at which the electron and ion fluxes were the same) was found to occur at a bias of −11 V. When the negative substrate bias was reduced (towards zero) from −11 V, electrons were preferentially attracted towards the substrate. As the substrate bias was made more negative than −11 V, positive ions were increasingly attracted towards the substrate. As shown in Appendix A (Eq. (A.3)), the collisionless acceleration of argon ions across the sheath held at the floating potential impacts the substrate with an energy that can be approximated as $0.5 \cdot T_e + e \cdot V_f$ where T_e is the electron temperature (eV) and V_f is the floating potential (V). For an electron in the 5–15 eV range and a substrate floating potential of −11 V, the ion impact energy lies in the 14–19 eV range.

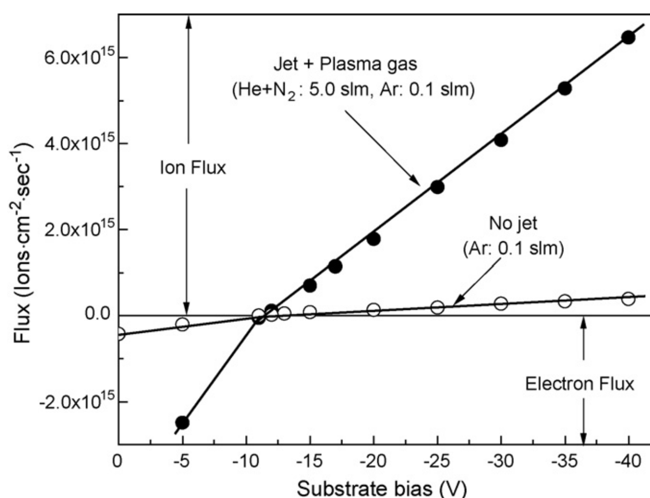

Fig. 3. Ion flux vs. substrate bias potential. The hollow cathode plasma generation process utilized argon as the working gas at flow rate of 0.1 slm. A nitrogen-doped helium gas jet with a flow rate of 5.0 slm was used to reactively synthesize lithium phosphorus oxynitride (Lipon) films from Li_3PO_4 vapor.

To determine the validity of the collisionless approximation, we note that the ion mean free path can be approximated [24]:

$$\lambda_{mfp} = \frac{5 \times 10^{-3}}{P}, \tag{1}$$

where λ_{mfp} is the vapor mean free path (cm) and P is the chamber pressure (Torr). During Lipon film synthesis, $P = 2.3 \times 10^{-2}$ Torr and so mean free path was approximately 2.0 mm. The plasma sheath thickness, d_{ps}, can be approximated by

$$d_{ps} \approx \left[\frac{e \cdot (V_p - V_s)}{T_e} \right]^a \cdot \lambda_D \tag{2}$$

where λ_D is the plasma Debye length (μm), V_p is the plasma potential (V), V_s is the substrate bias (V), T_e is the electron temperature (eV), and a is between 2/3 at high pressures and 3/4 at low pressures [24]. With the plasma potential (V_p) in the 40–100 V range, Eq. (2) indicates that the plasma sheath thickness, d_{ps}, is around 10 times smaller than the vapor mean free path. The collisionless approximation therefore appears to be valid and so the application of a substrate bias more negative than −11 V induces ion impact with the substrate and the ion impact energy will linearly increase with negative substrate bias as indicated by Eq. (A.6) in Appendix A.

3.3. Film characterization methods

The as-deposited Lipon films were characterized by scanning electron microscopy (SEM), X-ray diffraction (XRD), X-ray photoelectron spectroscopy (XPS), inductively coupled plasma optical emission spectroscopy (ICP-OES), and electrochemical impedance spectroscopy (EIS). Details of each experimental technique are given in our previous study [14].

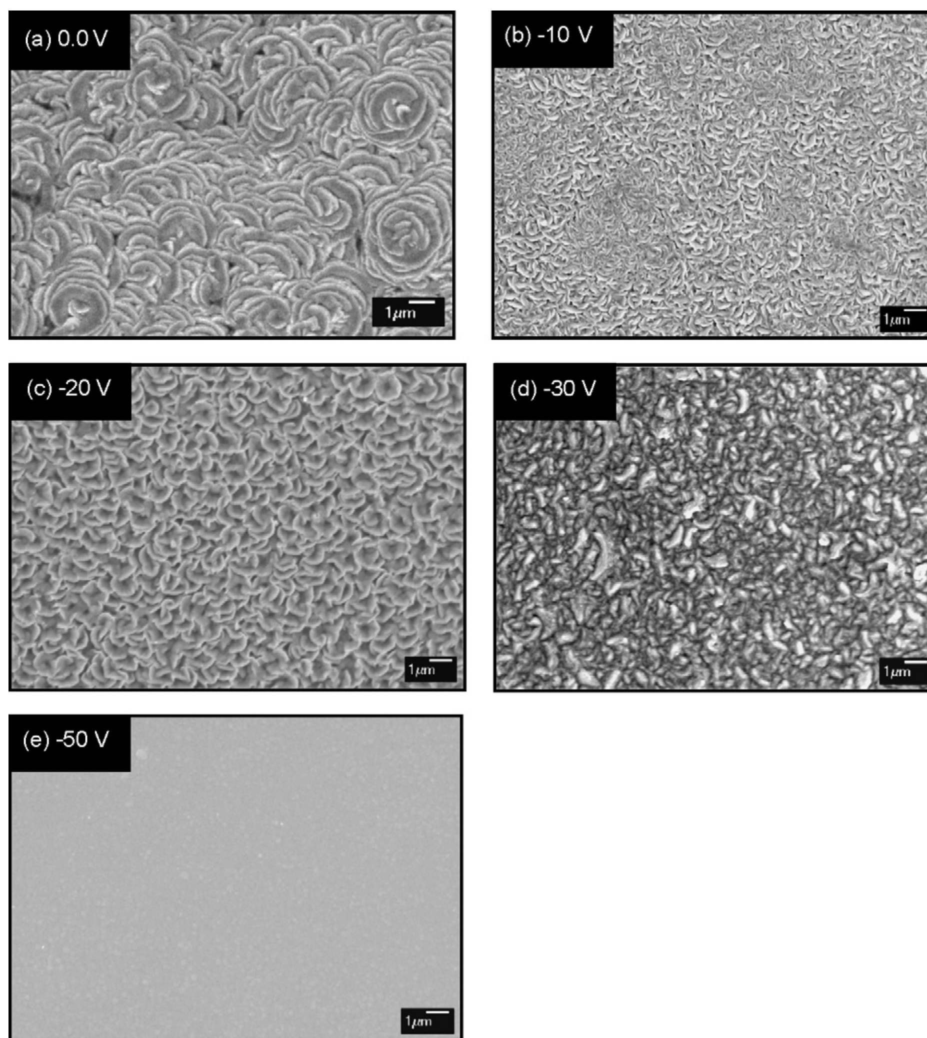

Fig. 4. (a–e) Surface morphologies of the Lipon films synthesized using negative substrate bias assistance.

4. Results and discussion

4.1. Film morphologies

When the Li_3PO_4 films were synthesized without the plasma assistance, they contained both cracks and pores because the high chamber pressure (7.5×10^{-3} –0.75 Torr) thermalized the vapor and broadened the angular incidence distribution [14,15,25]. Fig. 4 shows the surface morphologies of Lipon films synthesized using the plasma assistance with various substrate biases. When the substrate was grounded with plasma activation, Lipon films were deposited with spiral surfaces, Fig. 4(a). As the substrate bias was increased, the surface morphologies evolved to very smooth profile at a substrate of −50 V. Recent molecular dynamics simulations of low energy ion impacts with a film surface indicate that the surface smoothing increases with the argon ion flux and ion energy [26]. Fig. 3 shows that the ion fluxes linearly increased as a function of the negative substrate bias and Eq. (A.6) in Appendix A indicates that the ion energy also increases. This indicates that the surface smoothing is a result of low energy ion-assisted surface reconstruction, and the substrate bias voltage provides a means for the control of this effect during directed vapor deposition.

As the (heavy) argon ion impact energy increases, film sputtering can occur. Stuart et al. investigated the sputter yields of many materials subjected to argon ion impact. They found that the sputtering threshold energy of many materials lies in the 20–40 eV range [27]. The sputtering yield above this threshold was inversely proportional to the surface binding energy of materials [28]. During film growth, energetic ions impact surface adatoms that are not fully bonded to the surface and likely sputter them at below the sputtering threshold. During plasma-assisted deposition, we find that increases of the negative substrate bias potential decreased the Lipon film growth rate, Table 1. When film resputtering does not occur, low energy plasma assistance normally increases the deposition rate of films [29]. The reduction in overall deposition rate observed here as the ion impact energy/flux increased appears to be consequence of ion bombardment-induced film sputtering.

4.2. Film composition

The Li/P ratio in the Lipon films was measured by inductively coupled plasma optical emission spectroscopy (ICP-OES), Fig. 5. The shaded area in Fig. 5 shows the composition range reported for Lipon films synthesized by RF-magnetron sputtering approaches. These had Li/P ratio ranges of 2.4–4.2 and their Li-ion conductivities were in the 10^{-6} to 10^{-7} S cm^{-1} range [9,30,31]. Lipon films synthesized here without a bias voltage had a Li/P ratio similar to that of the sputter deposited films. Increasing the negative substrate bias

Table 1
Deposition rates and Li-ion conductivities of Lipon films synthesized using a negative substrate bias.

DC bias (V)	Film thickness (μm)	Deposition time (min)	Deposition rate ($nm\,min^{-1}$)	σ_{ionic} ($S\,cm^{-1}$)
0*	3.84	30	128	5.24×10^{-7}
−10	1.81	30	60.33	1.27×10^{-7}
−20	1.26	30	42.14	1.35×10^{-7}
−30	1.61	40	40.25	8.82×10^{-8}
−50	0.27	20	13.5	3.12×10^{-10}

The asterisk (*) indicated a result from previous work [14].

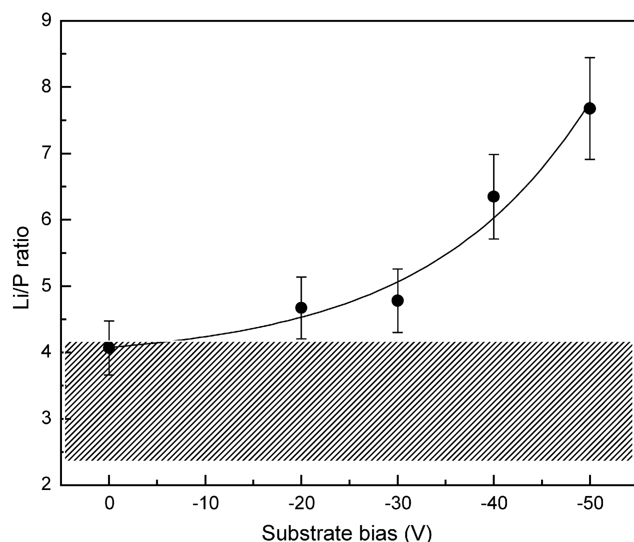

Fig. 5. The Li/P ratio dependence upon substrate bias for Lipon films synthesized using a plasma-assisted DVD approach. The Li/P ratio was determined by ICP-OES. The error bars are ±5% of the Li/P ratio. The shaded area shows the Li/P ranges (2.4–4.2) reported for films made by RF-magnetron sputtering approaches [6,30,31].

increased the Li/P ratio. Fig. 6 shows the P/N ratio of the films determined by XPS. The shaded area in Fig. 6 again indicates the P/N ratio (in the 0.74–6.25 range) of Lipon films prepared by RF-magnetron sputtering [9,30,31]. Once again, we find that films prepared here without a substrate bias had a similar P/N ratio to sputtered films. However, as the negative substrate bias was increased, the P/N ratio decreased and was significantly less than the range reported for sputtered films. The XPS and the ICP-OES results indicate that the phosphorus concentration of Lipon films decreases sharply with the substrate bias.

Because the preferential sputtering of elements is inversely proportional to their mass and surface binding energy, light elements are more preferentially sputtered than heavy elements [28]. In this study, as the negative substrate bias was increased, the Li/P ratio increased, and the P/N ratio decreased. The preferential sputtering theory of elements therefore fails to explain the present results. Using a RF-magnetron sputtering approach, Dudney et al. sputtered a Li_3PO_4 target by argon ions to synthesize Li_3PO_4 films [8]. They observed that the resulting films contained almost the target composition. This result indicates that argon ions might not preferentially sputter elements in the Li_3PO_4 targets. In the PA-DVD approach, the use of the negative substrate bias might accelerate ions towards the biased substrate surface. The ion velocity in the plasma sheath can be approximated by [17]:

$$u_i = \left(\frac{2q \cdot |V_{ps}|}{M_i}\right)^{1/2} \tag{3}$$

where u_i is the ion velocity ($m\,s^{-1}$), q is the ion charge, V_{ps} is the plasma sheath potential ($V_{ps} = V_p - V_{sb}$), V_p is the plasma potential (V), V_{sb} is the substrate bias (V), and M_i is the ion mass (kg). If a constant negative substrate bias is used and ions have the same charges, an ion velocity in the plasma sheath is inversely proportional to their mass, Eq. (3). Because lithium mass is 1.15×10^{-26} kg and phosphorus mass is 5.14×10^{-26} kg, lithium ions have higher velocity than phosphorus ions. Increasing the negative substrate bias would then accelerate more lithium ions towards the substrate

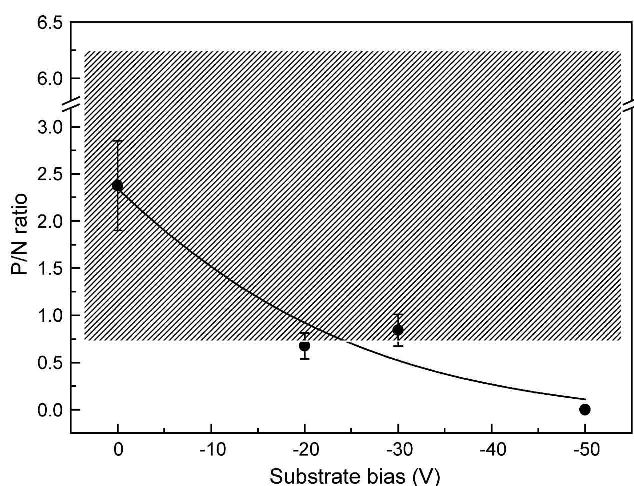

Fig. 6. P/N ratio in Lipon films deposited using a negative substrate bias. The P/N ratio was obtained by XPS. The error bars represent ±10% of the P/N ratio. The shaded area shows the P/N ranges (0.74–6.25) reported for samples made by RF-magnetron sputtering approaches [6,30,31].

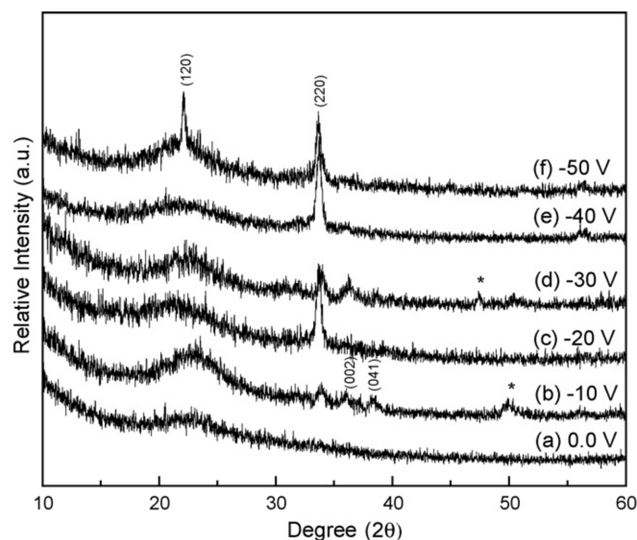

Fig. 7. X-ray diffraction patterns of Lipon films prepared using a substrate bias. There is a peak shift at a substrate bias of −30 V. The weak peaks marked as "*" are an unknown phase.

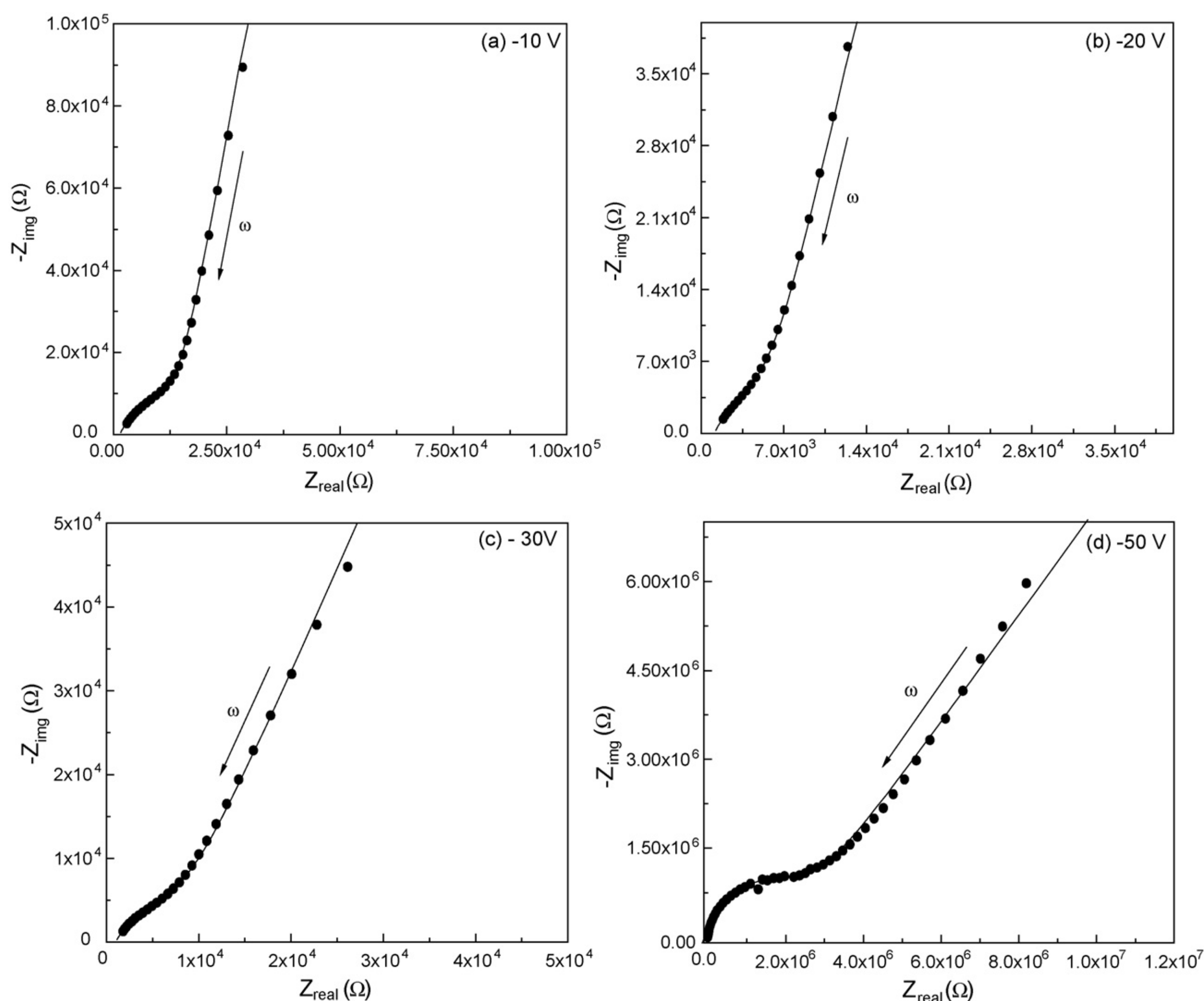

Fig. 8. EIS spectra of the Lipon films synthesized using a substrate bias of (a) −10 V, (b) −20 V, (c) −30 V and (d) −50 V. The frequency was scanned in the range of 1–10^5 Hz with 0.1 logarithmic increments and decreased along the direction of the arrow.

than phosphorus ions resulting in films with more lithium than phosphorus.

4.3. Film structure

X-ray diffraction (XRD) was used to analyze the structures of the Lipon films, Fig. 7. When the substrate bias was zero, the Lipon film had a broad peak without any evidence of local crystallinity. This is consistent with a Lipon film that was entirely amorphous. However, when the substrate bias between −10 V and −50 V was used, the Lipon films contained a broad peak and weak local crystalline peaks at (1 2 0), (2 2 0), and (0 0 2) reflections of the Li_3PO_4 phase. The presence of both the broad peaks and the crystalline peaks indicates that Lipon films included regions of a local crystallinity in an amorphous matrix. The result is analogous to that of Martin et al. who synthesized ZrO_2 films by an e-beam evaporation while bombarding the growing film surface with argon ions [32]. They found that their ZrO_2 films when bombarded by argon ions had a crystalline structure while e-beam evaporated ZrO_2 films were amorphous without a substrate heating. Because the negative substrate bias increased the surface atomic mobility, it facilitated formation of local regions of crystallinity within these Lipon films.

4.4. Li-ion conductivity

Fig. 8 shows EIS spectra of the Lipon films measured by the same approach used in the earlier study [14]. The Li-ion conductivities are shown in Table 1. It can be seen that they decreased from 10^{-7} S cm^{-1} to 10^{-10} S cm^{-1} as the substrate bias was increased. Bates et al. observed that when nitrogen atoms were incorporated into the Li_3PO_4 structure, the Li-ion conductivities of amorphous Lipon films increased from 10^{-8} S cm^{-1} to 10^{-6} S cm^{-1} [7]. In polycrystalline Lipon materials, nitrogen incorporation increased the average Li–O atomic distance [33]. Because this weakened the Li–O bond energy and also increased the area of triangular faces of the tetrahedral site where lithium ions reside, the incorporation of nitrogen reduces the activation energy for lithium ion migration from 0.67 eV to 0.54 eV in Lipon films. Lithium ions can therefore more easily move in Lipon films and the resulting Li-ion conductivity increases with the nitrogen incorporation. In the experiment reported here, Li-ion conductivities gradually decreased because the negative substrate bias created local crystalline peaks in Lipon films, Fig. 7. Even though Lipon films contained only localized crystallinities, the use of substrate bias of between −20 V and −30 V resulted in Li-ion conductivities in the 10^{-7} S cm^{-1} range. As indicated by Park et al., while not ideal, Li-ion conductivities were still

within the acceptable range for rechargeable thin-film Li/Li-ion batteries [14,34].

5. Conclusions

The effects of a negative substrate bias upon the PA-DVD synthesis of Lipon electrolyte films for rechargeable thin-film Li/Li-ion batteries have been investigated. Bias-assisted deposition created local regions of crystallinity in an amorphous Lipon matrix and modified surface morphologies of the films from spiral to a spiral-free smooth pattern. During film deposition, a negative substrate bias increased the surface atomic mobility by accelerating either ionized vapor atoms and/or gas ions toward the substrate and this affected the fraction of the crystalline phase and the morphology of the films. Increase of the negative substrate bias also enhanced ion bombardment of the film's growth surface, which led to film sputtering and a decreased Lipon film deposition rate. The use of negative substrate bias appears to preferentially accelerate light lithium ions, which increased the Li/P ratio in the films. Increasing the substrate bias also lowered the Li-ion conductivities because it promoted crystallization of the Lipon films. Li-ion conductivities of Lipon films were in the range of 10^{-7} to 10^{-10} S cm^{-1}, with those in the 10^{-7} S cm^{-1} range remaining acceptable for some rechargeable thin-film batteries.

Acknowledgements

I would like to thank Carol Holden for her assistance with using the inductively coupled plasma optical emission spectroscopy (Virginia Commonwealth University, USA). I am also thankful to Dr. Cathy Duke for training in X-ray photoelectron spectroscopy (University of Virginia, USA).

Appendix A

When a substrate is floated in a plasma, their surface is negatively charged by electrons because electrons move into the substrate much faster than ions. In this manner, the substrate forms a floating potential where the substrate has the same flux of both electrons and ions. This floating potential creates a plasma pre-sheath and plasma sheath near the substrate. Because ions are initially accelerated through the plasma pre-sheath, their energy can be estimated at the plasma sheath edge by ion velocity (u_{is}), which is provided by Bohm sheath criterion condition. This Bohm sheath criterion condition is given by [17]:

$$u_{is} \geq u_B = \left(\frac{T_e}{M_i}\right), \tag{A.1}$$

where u_B is the Bohm velocity (m s^{-1}), T_e is the electron temperature (eV), and M_i is the ion mass (kg). Eq. (A.2) indicates that ions have the Bohm velocity (u_B) at the plasma sheath edge. The ion velocity can be converted into the ion energy (E_{is}) as follows [17]:

$$E_{is} = \frac{1}{2}\cdot M_i \cdot u_{is}^2 \geq \frac{1}{2}\cdot M_i \cdot u_B^2 = \frac{1}{2}T_e. \tag{A.2}$$

At the plasma sheath edge, the ion energy becomes half of the electron energy or greater.

If ions arrive at the plasma pre-sheath edge, they will be accelerated to the plasma sheath edge with the Bohm velocity and then accelerated through the plasma sheath by the plasma sheath potential. When the accelerated ions hit a surface of the floating substrate, their energy, E_{if}, is approximately proportional to a floating potential as follows [17]:

$$E_{if} = E_{is} + V_f \tag{A.3}$$

$$= \frac{1}{2}\cdot T_e + \left| -T_e \cdot \ln\left(\frac{M_i}{2\pi \cdot m_e}\right)^{1/2} \right|, \tag{A.4}$$

where V_f is the floating potential, T_e is the electron temperature (eV), M_i is the ion mass (e.g., Ar = 6.64×10^{-26} kg), and m_e is the electron mass (9.11×10^{-31} kg).

If a substrate is negatively biased, then ions will be attracted into the substrate by a plasma sheath potential (V_{ps}) and the ion current (j_i) is represented by [17]:

$$j_i = \frac{4}{9}\cdot \varepsilon_o \cdot \left(\frac{2e}{M_i}\right)^{1/2} \cdot \frac{(V_{ps})^{3/2}}{d_{ps}^2}, \tag{A.5}$$

where $V_{ps} = V_p - V_{sb}$, V_p is the plasma potential (V), V_{sb} is the substrate bias (V), M_i is the ion mass, ε_o is the dielectric constant (8.84×10^{-14} F cm^{-1}), and d_{ps} is the plasma sheath thickness (mm). In this case, the ion kinetic energy (E_i) at a substrate surface is approximately proportional to the applied negative bias (V_{sb}) [17]:

$$E_i \cong \frac{1}{2}\cdot T_e + e \cdot V_{sb} \tag{A.6}$$

As shown in Eqs. (A.5) and (A.6), if a negative bias is applied to the substrate, then it will increase the substrate ion current and the ion energy. This substrate bias will increase ion bombardments onto the substrate, which can modify a surface morphology and a composition. In these aspects, ion plating has been used to control the properties of films such as film density, film adhesion, and film composition [18,35,36].

References

[1] S.D. Jones, J.R. Akridge, J. Power Sources 54 (1995) 63–67.
[2] J.M. Tarascon, M. Armand, Nature 414 (2001) 359–367.
[3] S.W. Jin, H.N.G. Wadley, J. Vacuum Sci. Technol. A: Vacuum, Surf. Films 26 (2008) 114–122.
[4] N.J. Dudney, J.B. Bates, R.A. Zuhr, S. Young, J.D. Robertson, H.P. Jun, S.A. Hackney, J. Electrochem. Soc. 146 (1999) 2455–2464.
[5] D. Linden, T.B. Reddy, Handbook of Batteries, McGraw-Hill, New York, 2002.
[6] P.G. Bruce, Solid State Electrochemistry, Cambridge University Press, 1997.
[7] J.B. Bates, N.J. Dudney, G.R. Gruzalski, R.A. Zuhr, A. Choudhury, C.F. Luck, J.D. Robertson, Solid State Ionics 53–56 (1992) 647–654.
[8] N.J. Dudney, J.B. Bates, J.D. Robertson, J. Vacuum Sci. Technol. A: Vacuum, Surf. Films 11 (1993) 377–389.
[9] X. Yu, J.B. Bates, J.G.E. Jellison, F.X. Hart, J. Electrochem. Soc. 144 (1997) 524–532.
[10] Y. Hamon, A. Douard, F. Sabary, C. Marcel, P. Vinatier, B. Pecquenard, A. Levasseur, Solid State Ionics 177 (2006) 257–261.
[11] S. Zhao, Z. Fu, Q. Qin, Thin Solid Films 415 (2002) 108–113.
[12] W.-Y. Liu, Z.-W. Fu, C.-L. Li, Q.-Z. Qin, Electrochem. Solid-State Lett. 7 (2004) J36–J40.
[13] F. Vereda, R.B. Goldner, T.E. Haas, P. Zerigian, Electrochem. Solid-State Lett. 5 (2002) A239–A241.
[14] Y.G. Kim, H.N.G. Wadley, J. Vacuum Sci. Technol. A: Vacuum, Surf. Films 26 (2008) 174–183.
[15] J.F. Groves, Ph.D. Dissertation, University of Virginia, Charlottesville, 1998.
[16] Y.G. Kim, H.N.G. Wadley, Solid State Ionics (submitted for publication).
[17] M.A. Lieberman, A.J. Lichtenberg, Principles of Plasma Discharges and Materials Processing, John Wiley & Sons Inc., 1994.
[18] D.M. Mattox, Electrochem. Technol. 2 (1964) 295.
[19] D.M. Mattox, Handbook of Physical Vapor Deposition (PVD) Processing, William Andrew Publishing/Moyes Publications, 1998.
[20] O. Zywitzki, K. Goedicke, H. Morgner, Surf. Coat. Technol. 151–152 (2002) 14–20.
[21] H. Morgner, M. Neumann, S. Straach, M. Krug, Surf. Coat. Technol. 108–109 (1998) 513–519.
[22] S. Schiller, V. Kirchhoff, N. Schiller, H. Morgner, Surf. Coat. Technol. 125 (2000) 354–360.
[23] S. Schiller, C. Metzner, O. Zywitzki, Surf. Coat. Technol. 125 (2000) 240–245.
[24] M. Ohring, Materials Science of Thin Films: Deposition and Structure, Academic Press, San Diega, CA, 2002.
[25] D.D. Hass, Ph.D. Dissertation, University of Virginia, Charlottesville, 2000.
[26] J.J. Quan, X.W. Zhou, H.N.G. Wadley, Surf. Sci. 600 (2006) 4537–4547.
[27] R.V. Stuart, G.K. Wehner, J. Appl. Phys. 33 (1962) 2345–2352.
[28] P. Sigmund, Spttering by Particle Bombardment. I. Physical Sputtering of Single Element Solids, Springer, New York, 1981.
[29] J.M.E. Harper, J.J. Cuomo, R.J. Gambino, H.R. Kaufman, Nucl. Instrum. Methods Phys. Res. B: Beam Interact. Mater. Atoms 7–8 (1985) 886–892.

[30] C.H. Choi, W.I. Cho, B.W. Cho, H.S. Kim, Y.S. Yoon, Y.S. Tak, Electrochem. Solid-State Lett. 5 (2002) A14–A17.
[31] N.J. Dudney, M.L. Jenson, Properties of Vacuum Deposited Thin Films of Lithium Phosphorus Oxynitride (Lipon) with an Expanded Composition Range, Oak Ridge National Laboratory, Oak Ridge, 2003.
[32] P.J. Martin, R.P. Netterfield, W.G. Sainty, J. Appl. Phys. 55 (1984) 235–241.
[33] B. Wang, B.C. Chakoumakos, B.C. Sales, B.S. Kwak, J.B. Bates, J. Solid State Chem. 115 (1995) 313–323.
[34] H. Park, S. Nam, Y. Lim, K. Choi, K. Lee, G. Park, S.-R. Lee, H. Kim, S. Cho, J. Electroceram. 17 (2006) 1023–1030.
[35] D.M. Mattox, J. Vacuum Sci. Technol. 10 (1973) 47–52.
[36] D.M. Mattox, G.J. Kominiak, J. Vacuum Sci. Technol. 9 (1972) 528–532.